

SIMULATION STUDY OF THE HELICAL SUPERCONDUCTING UNDULATOR INSTALLATION AT THE ADVANCED PHOTON SOURCE*

V. Sajaev, M. Borland, Y.-P. Sun, A. Xiao, ANL, Argonne, IL 60439, USA

Abstract

A helical superconducting undulator is planned for installation at the APS. Such an installation would be first of its kind, since a helical undulator was never installed in synchrotron light source before. Due to its reduced horizontal aperture, a lattice modification is required to accommodate large horizontal oscillations during injection. We describe details of the lattice change and show results of experimental tests of the new lattice. To understand the effect of the undulator on single-particle dynamics, we first computed kick maps using different methods. We have found that often-used Elleaume formula [1] for kick maps gives incorrect results for this undulator. We then used the kick maps obtained by other methods to simulate the effect of the undulator on injection and lifetime.

INTRODUCTION

Advanced Photon Source has been methodically developing superconducting undulators (SCU) for a number of years. Presently, two planar SCUs are in operation at APS [2]. As a next step, a helical superconducting undulator is in development, with installation planned for next year [3]. The main parameters of the undulator are given in Table 1. In an ordinary planar undulator, the vertical gap of the vacuum chamber is usually made as small as possible to reduce the distance between the magnet arrays and to increase the vertical magnetic field, while the horizontal gap is not important and is usually made comparatively large. This works well for the traditional injection design where large horizontal acceptance is required to capture the injected beam. In a helical undulator, the poles and coils form a circle around the vacuum chamber, and therefore both vertical and horizontal aperture is small. With a horizontal inside diameter of of 26

Table 1: Main Parameters of the Helical SCU

Cryostat length	1.85 m
Magnetic length	1.2 m
Undulator period	31.5 mm
Undulator field $B_x = B_y$	0.4 T
Undulator parameter	1.2
Magnetic bore diameter	31 mm
Full vacuum chamber gap	26 × 8 mm

mm, the helical undulator will become the smallest aperture in the ring. To avoid reduction of the horizontal acceptance, the beta functions at the SCU location must be changed.

* Work supported by the U.S. Department of Energy, Office of Science, Office of Basic Energy Sciences, under Contract No. DE-AC02-06CH11357.

In this paper, we describe the required lattice modification and simulate the effect of the helical undulator on the beam dynamics.

LATTICE MODIFICATIONS

The original APS lattice is made of 40 nearly-identical sectors, each of which has a 5-m-long straight section for insertion device (ID) installation. The Twiss parameters at the standard ID center are $\beta_x = 19.5$ m, $\beta_y = 2.9$ m, and $\eta_x = 0.17$ m. To better serve the user program at sector 32, a few years ago the beta functions there were modified to $\beta_x = 3.6$ m, $\beta_y = 5.0$ m, and $\eta_x = 0.07$ m, which allowed for the horizontal beam size reduction by a factor of 2.3. The effect of this single-sector symmetry breaking on the nonlinear dynamics was minimal and did not require any special sextupole optimization. This lattice is now in operation full time.

From the previous experience with planar SCUs we know that excessive beam losses at the SCU location can lead to magnet quenches [4]. Since the HSCU horizontal gap of ± 13 mm will be the smallest horizontal physical aperture in the ring, to avoid beam losses inside the device the beta functions must be modified to increase acceptance at this location. The following conditions were considered for lattice modification: (1) the HSCU vacuum chamber extends from +0.7 m to +2.2 m relative to the center of the sector 7 straight section and has a gap of ± 13 mm \times ± 4 mm; (2) the HSCU chamber acceptance should be larger than the two smallest existing acceptances; (3) the smallest existing acceptance is sector 4 ID chamber with gap of ± 15 mm \times ± 2.4 mm that extends from -2.5 m to +2.5 m relative to the center of the ID straight section; (4) the second smallest acceptance is a number of ID chambers with gap of ± 18 mm \times ± 3.5 mm that have the same length as the sector 4 chamber; (5) the horizontal dispersion at HSCU needs to scale with the horizontal limiting aperture locations (ID4 and other IDs) to preserve Touschek lifetime; (6) the modified beta functions should deviate from the standard sectors as little as possible.

A lattice that satisfies all the above conditions was designed using the optimizer in `elegant` [5]. The lattice functions at the entrance of sector 7 were fixed, and all 10 quadrupoles in sector 7 were used in optimization. The quadrupoles in sector 8 were then set to provide mirror symmetry around the end of sector 7 (middle of the sector 7 ID straight section) to return the lattice functions back to the original values at the exit of sector 8. The lattice functions of sectors 7 and 8 are shown in Figure 1. The drift spaces at the left and right ends of the plot correspond to the standard ID straight sections while the drift space in the middle of the plot is the straight section with modified beta functions.

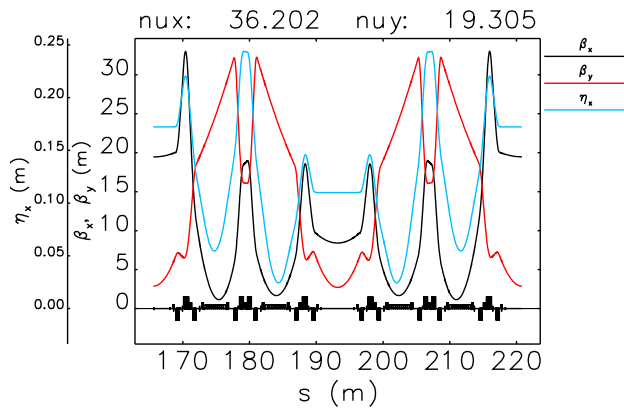


Figure 1: Twiss parameters of the modified sector 7 and 8. ID straight section is in the middle of the plot.

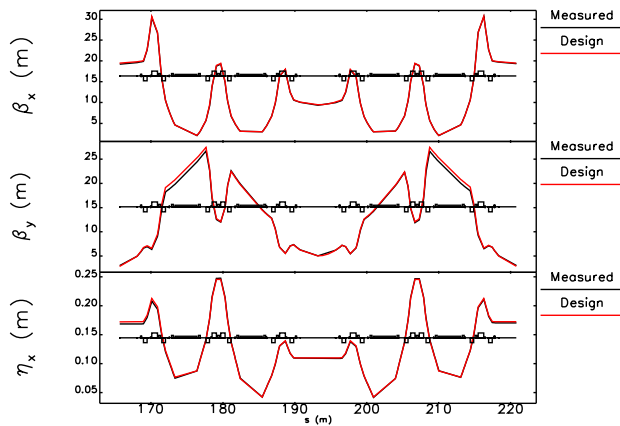


Figure 2: Comparison between the designed and measured optics functions in sectors 7 and 8.

The optimized lattice was tested in beam studies. APS operates in several fill patterns with two significantly different sets of chromaticities: uniform fill patterns of 24 and 3424 bunches are operated with chromaticity of $\sim +3$ in both planes, while asymmetric hybrid mode has chromaticities of $+11$ to allow for accumulation of 16-mA high-charge camshaft bunch. This later condition is obviously more demanding in terms of nonlinear dynamics, hence we used it for our tests. The design lattice parameters were achieved without any lattice correction, as shown in Figure 2.

The effect of the lattice modification on the lifetime was rather significant – the lifetime was reduced by about a factor of two. This was a surprising result since the beta function change in this lattice was not as drastic as those in sector 32 that were described above. An offline tracking-based multi-objective genetic optimization [6, 7] of sextupole strengths was performed to improve the lifetime. The optimization varied sextupoles in 21 families – 7 families per standard sector plus 14 sextupoles around sector 4 ID where the smallest physical aperture is located. The optimization objectives were dynamic aperture and local momentum aperture. Using sextupoles obtained in the optimization, we were able to almost fully recover the lifetime (from 200 to 350 minutes),

which is acceptable to topup operation. The injection efficiency after optimization remained acceptable too at 75%.

EFFECT ON BEAM DYNAMICS

Over the past years, several methods were developed for studying beam dynamics in the presence of insertion devices. Some of these methods are encoded in *elegant* in elements called CWIGGLER, GFWIGGLER and UKICKMAP. In principle, the CWIGGLER and GFWIGGLER can be used for a general ID field, but the current implementation is only applicable to an insertion device with planar poles because they use the Halbach-like expansion of the magnetic field, with the scalar potential written by:

$$V = \sum_{m,n} -C_{m,n} \cos(K_{x,m,n}x) \sinh(K_{y,m,n}y) \cos(K_n z + \phi_n). \quad (1)$$

The UKICKMAP is a more general element; its input can be derived from a magnet design code, analytical formula such as P. Elleaume's method [1], or other direct tracking method, such as FTABLE in *elegant*.

For the helical SCU, the magnetic field in the body of the magnet can be expressed as (see Equation A.9 in [8]):

$$\begin{aligned} B_x &= B_0 \left\{ \left[1 + \frac{k^2}{8}(3x^2 + y^2) \right] \sin kz - \frac{1}{4}k^2xy \cos kz \right\} \\ B_y &= -B_0 \left\{ \left[1 + \frac{k^2}{8}(x^2 + 3y^2) \right] \cos kz - \frac{1}{4}k^2xy \sin kz \right\} \\ B_z &= B_0 \left\{ \left[1 + \frac{k^2}{8}(x^2 + y^2) \right] (kx \cos kz + ky \sin kz) \right\} \end{aligned} \quad (2)$$

where $k = 2\pi/\lambda$ is the wavenumber and B_0 is the on-axis maximum field. One can see that the HSCU field is very different from the field of a planar device shown in Equation 1 (which also covers an APPLE device that has 4 rows of planar poles). Instead of changing the existing code, we decide to use other methods.

To compare different methods to generate the kick maps, we used three approaches: P. Elleaume formula, the FTABLE element, and direct numerical integration of the magnetic fields given in equation (2) using the general equations of motion. As was mentioned before, the expressions (2) only describe the field inside the undulator but not on the edges of the device. We could not find any published expressions for the edge field of helical undulator, therefore, we used the same expressions as in (2) for the edges but with B_0 linearly ramping from 0 to maximum over the length of the edge. We understand that Maxwell equations are not satisfied in this assumption and discuss this later in more detail. Figure 3 compares the $x-x'$ kick maps for particle with $y=0$ calculated through the entire device with edges included (two periods per edge). One can see a significant discrepancy between the P. Elleaume method and the direct integration.

The detailed HSCU kick map calculated using FTABLE is shown in Figure 4. From the calculated kick map, one can see that the major perturbation terms from the

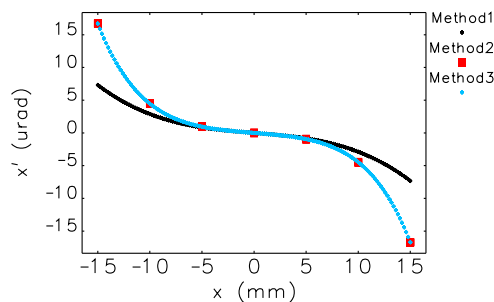


Figure 3: Calculated kick map for HSCU using field from (2). Method 1 is P. Elleaume integration, methods 2 and 3 are direct numerical integration and FTABLE.

HSCU are quadrupole and octupole terms. The fitted terms are $\int(dB_y/dx)ds = -50$ G; $\int(dB_x/dy)ds = -40$ G; $\int(d^3B_y/dx^3)ds = -160$ G/cm² and $\int(d^3B_x/dy^3)ds = -51$ G/cm². The kick map given by these fitted integrated multipoles is shown in Figure 5 and agrees well with the kick map from 4, which means that this set of multipoles represents well the integrated effect of the helical SCU on the beam.

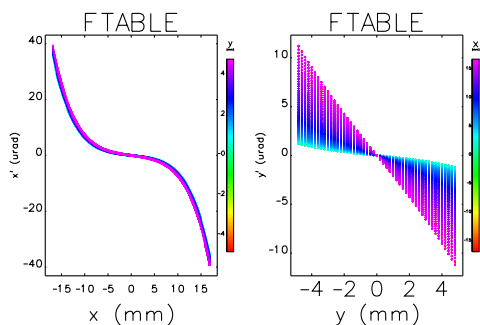


Figure 4: Calculated detailed kick map for HSCU. Color code is the other coordinate (for example, y for the left plot)

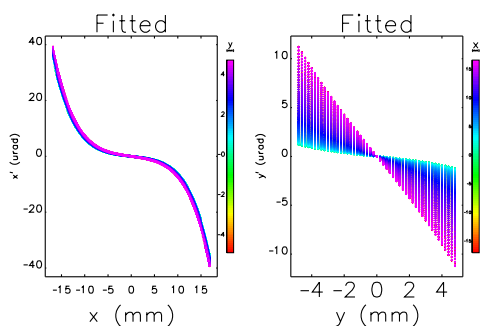


Figure 5: Kick map calculated using fitted multipole components.

The beam dynamics was simulated with and without HSCU for 8 random sets of lattice errors. The tracking

was performed using `elegant` and the kickmap calculated from FTABLE. The resulting median value of simulated dynamic aperture and momentum aperture are shown in Figure 6. There is no noticeable reduction of dynamic or momentum aperture when HSCU is added to the lattice, therefore the HSCU should present no significant effect of lifetime and injection efficiency.

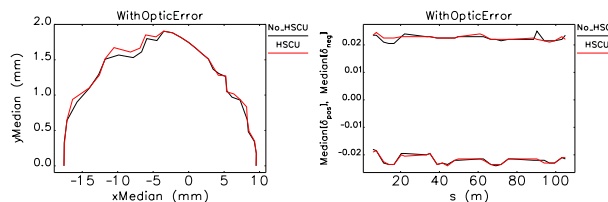


Figure 6: Comparison of dynamic aperture with (red) and without (black) HSCU (left) and local momentum aperture (right).

As was mentioned before, our assumption for the edge treatment does not satisfy Maxwell's equations. We may assume that if the field ramp with z was much slower, the errors introduced by our assumption would be much smaller too. To test this, we compared kick maps with different numbers of periods used for ramping the field, finding no difference in the kick maps. Even though it is not the solid indication that the edges are treated correctly, it is an indication that edge effects are weak.

CONCLUSIONS

We have designed and tested a lattice that will allow for installation of the helical superconducting undulator with small horizontal aperture in the APS storage ring (planned for late 2017). We have also simulated the effect of this undulator on the nonlinear beam dynamics and found no significant effect.

REFERENCES

- [1] P. Elleaume, in *Proc. EPAC 1992*, pp. 661–663.
- [2] Y. Ivanushenkov *et al.*, *Phys Rev ST Accel Beams (in press)*, vol. 18, p. 040703, 2015.
- [3] Y. Ivanushenkov, *et al.*, presented at *NA-PAC 16*, paper THA1CO06, this conference.
- [4] K. Harkay, *et al.*, in *Proc. ICAP 2015*, paper TUPJE066.
- [5] M. Borland, ANL/APS LS-287, Advanced Photon Source, 2000.
- [6] I. Bazarov *et al.*, *Phys Rev ST Accel Beams*, vol. 8, p. 034202, 2005.
- [7] M. Borland *et al.*, ANL/APS/LS-319, APS, 2010.
- [8] S. Kim, *NIM A*, vol. 584, p. 266, 2008.